

Precise Evaluation of Positioning Repeatability of MR-Compatible Manipulator Inside MRI

Yoshihiko Koseki¹, Ron Kikinis², Ferenc A. Jolesz², and Kiyoyuki Chinzei¹

¹ National Institute of Advanced Industrial Science and Technology,
1-2-1 Namiki, Tsukuba, Ibaraki 305-8564, Japan
<http://unit.aist.go.jp/humanbiomed/surgical/>

² Department of Radiology, Brigham and Women's Hospital,
Francis St. 75, Boston, MA 02115, USA
<http://splweb.bwh.harvard.edu:8000/>

Abstract. In this paper, we experimentally tested the positioning repeatability of MR-compatible manipulator with a CCD laser micrometer inside MRI. To evaluate the performance of MR-compatible manipulator inside MRI, the measuring system must be confirmed to work correctly inside MRI in advance. Therefore, the measuring system was tested to see if it can measure a specimen similarly regardless to inside or outside MRI. The results inside MRI were different from those outside MRI but the differences were small in comparison with the typical error of our manipulator. With this measuring system, the positioning repeatability of our MR-compatible manipulator was tested inside MRI with image sequence, inside MRI without image sequence, and outside MRI. The results proved that the manipulator performed 0.17[mm] translational and 0.17[deg] rotational positioning repeatability on average, whether inside or outside MRI, whether with or without image sequence.

1 Introduction

1.1 Robotic Assist for MR-Guided Surgery

It has been said for a long time that the combination of intraoperative tomography and robot would promote less invasive surgery, because a manipulator which is numerically controlled referring to the coordinate of tomography can precisely position a surgical tool to a tumor behind normal tissue. In particular among medical tomography, MRI is superior to X-ray CT in terms of its good soft tissue contrast, lack of ionizing radiation, and potential of functional imaging. Therefore, many researchers have been studying MR-compatible robotics, which can work inside and/or nearby MRI.

Masamune has proposed one for stereotactic neurosurgery since 1995[1]. We also have studied MR-compatible mechanics and electronics since 1996 to develop not only robotic manipulators but also other devices, which can work nearby MRI[2]. We have developed 5 d.o.f (degrees of freedom) manipulator for brachytherapy of prostate cancer[3], 6 d.o.f one for general purpose[4], and 4 d.o.f one for trans-nasal neuro-surgery in vertical field open MRI[5]. Kaiser also has proposed one for stereotactic biopsy and therapy of breast cancer since 2000[6].

1.2 Evaluations of MR-Compatible Manipulator Inside MRI

Not only the development of MR-compatible manipulator, but the methods to evaluate it are also important. MRI's electromagnetic phenomena are static magnetic field B_0 , dynamic magnetic field B_1 , and image sequence (RF-pulse sequence). B_1 and image sequence might cause error on sensors and actuators of feedback loop. A movement of a metallic part in B_0 induces resistance force against the movement. Such complications between multi d.o.f manipulator and MRI make it difficult to predict the performance of the manipulator. Therefore, the final performance of MR-compatible manipulator under the influence of MRI's strong magnet must be tested inside MRI.

Measuring the manipulator's performance inside MRI is technically as difficult as developing an MR-compatible manipulator, because the measuring system itself is also under the influence of strong magnet, therefore requires validation of MR compatibility.

1.3 Our Approach

In this paper, we have studied the positioning repeatability of our MR-compatible manipulator inside MRI, because positioning repeatability is one of the most important performances of robot but it has never been precisely measured inside MRI to the extent of the authors' knowledge. This paper is composed from two experiments, the first is validation of the MR-compatibility of our measuring system, and the second is the robot test. A CCD laser micrometer was tested to see if it can measure a specimen similarly regardless to inside or outside MRI. After that, the repeatability of our MR-compatible manipulator was tested in same conditions. The results proved that the manipulator performed 0.17[mm] translational and 0.17[deg] rotational positioning repeatability on average, whether inside or outside MRI, whether with or without image sequence.

2 Materials and Methods

2.1 Measurement System Pretests

A CCD laser micrometer, VG-035/300 (KEYENCE, Osaka, Japan) was used for measurement. It is a pair of laser projector and receiver, and a cylindrical object is placed between them. The projector beams a sheet of laser and the receiver, a line CCD sensor detects the object's shadow. The CCD can detect the edge(s) of the object's shadow. VG-035/300 can measure the position and diameter of the object on the same basics. The summary specifications of VG-035/300 are described in Table 1.

A brass cylinder was prepared and measured by VG-035/300 inside MRI with image sequence, inside MRI without image sequence, and outside MRI. The reference cylinder and sensor heads were set in the gantry of intraoperative MRI, Signa SPTM(GE Medical Systems, Milwaukee, WI, 0.5 Tesla). Signa SP has two magnets with 0.5[m] horizontal opening. Each magnet has an inside

Table 1. Summary specifications of KEYENCE VG-035/300 from its catalog

Sensor head	VG-035
Controller	VG-300
Measuring area	35mm
Repeatability	5 μ m
Projector-receiver distance	0 to 300mm
Light source	Semiconductor laser (670nm, 38 μ W, pulse duration: 641 μ s)
CCD	Resolution: 5000bit
Sensor head's material	Die-cast aluminum

Table 2. Parameters of the MRI and the pulse sequence

Center frequency	21MHz	Bandwidth	62.5Hz
Sequence	Fast spin echo	Repetition time	1200ms
Echo time	96ms	Slice thickness	3.7mm
Matrix	256 \times 256	Resolution	1.4mm ²

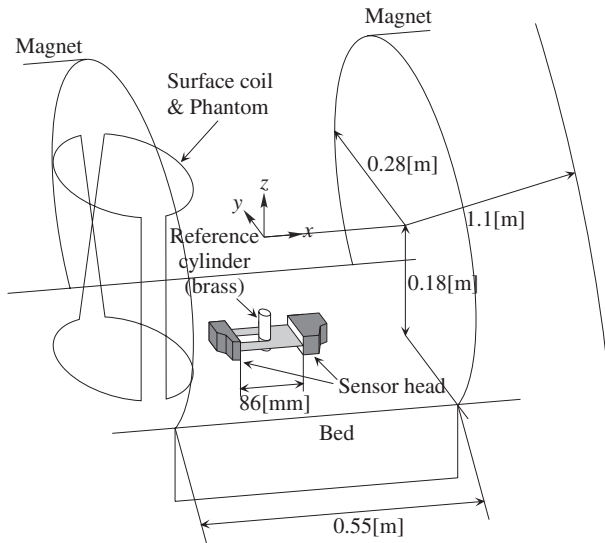


Fig. 1. Setup of measurement system pretest: arrangement of brass cylinder, sensor head, surface coil and phantom inside the gantry of GE's intraoperative MRI

diameter of 0.5[m] and outside diameter of 2.2[m]. The parameters of the MRI and the pulse sequence were shown in Table 2.

Inside the MRI, the reference cylinder was put vertically on the bed. The sensor heads were put horizontally on the bed. A surface coil and phantom

were put on the end of imaging area avoiding the conflict with the cylinder and measuring system. In this test, applying image sequence was necessary but MRI imaging was not. However, MRI canceled the image sequence by detecting the absence of the surface coil and phantom. The geometrical setup is shown in Fig. 1. The diameter was measured 30 times for each condition.

2.2 Repeatability Tests of MR-Compatible Manipulator

For the manipulator examination, we used 6 d.o.f manipulator using leverage and parallelogram mechanism introduced in [4]. The leverage and parallelogram mechanism can transmit 3 translational and 3 rotational motions from the outside to the inside of MRI. This remote actuation enables the less MR-compatible and bulky driving units to be set away from MRI.

The driving units form a fixed-linear parallel mechanism, and are set beside the surgical bed, between magnets of Signa SP, above the surgeon. The kinematic parameters are decided to meet the translational workspace of ± 100 [mm], and rotational workspace of ± 30 [deg].

The linear actuator unit of parallel mechanism consists of ultrasonic motor (USR60-S3N: Shinsei Kogyo Corp., Tokyo, Japan), linear encoder (LM 25CPMM-3S: 0.01[mm] resolution after $\times 4$, Encoder Technology, CA, USA), and limit & home switch (EE-SV3: Omron, Kyoto, Japan). The electrical signals of linear encoder are optically transmitted to the outside of operation room.

The repeatability of our MR-compatible manipulator was tested inside MRI with image sequence, inside MRI without image sequence, and outside MRI. The image sequence parameters were same as before (see Table 2).

VG-035/300 can measure only 1 d.o.f. at a time. Fig. 2 shows how 6 d.o.f were measured with two sets of VG-035/300. The coordinate systems of the manipulator and the manipulator's tool holder were assumed to match that of MRI (See Fig. 1). A long bakelite bar was attached to the tool holder of the manipulator in parallel to x -axis of the tool holder. One set of VG-035/300 measured z -axis position of one point on the bar (a_x in Fig. 2), and the other set measured z -axis position of the different point (b_x in Fig. 2). The sensor heads were fixed on a precisely machined acrylic block, therefore the gap between two sets, $(x_2 - x_1)$, $(y_2 - y_1)$, and $(z_2 - z_1)$ and the gap between sensor heads, d_1 were relatively precise. The bakelite bar and the acrylic block were aligned manually so that the bakelite and the direction of $(x_2 - x_1)$ were parallel to x -axis of MRI. x_1 , y_1 , and z_1 had to be measured by a ruler. Therefore they were relatively imprecise.

The translational positioning error in z -axis and rotational positioning error around y -axis are calculated as the following equations. Hereafter, E_x , E_y , and E_z are translational positioning errors in x -, y -, and z -axis, respectively. E_p , E_q , and E_r are rotational positioning errors around x -, y -, and z -axis, respectively. $STDEV(a)$ is the standard deviation of group a .

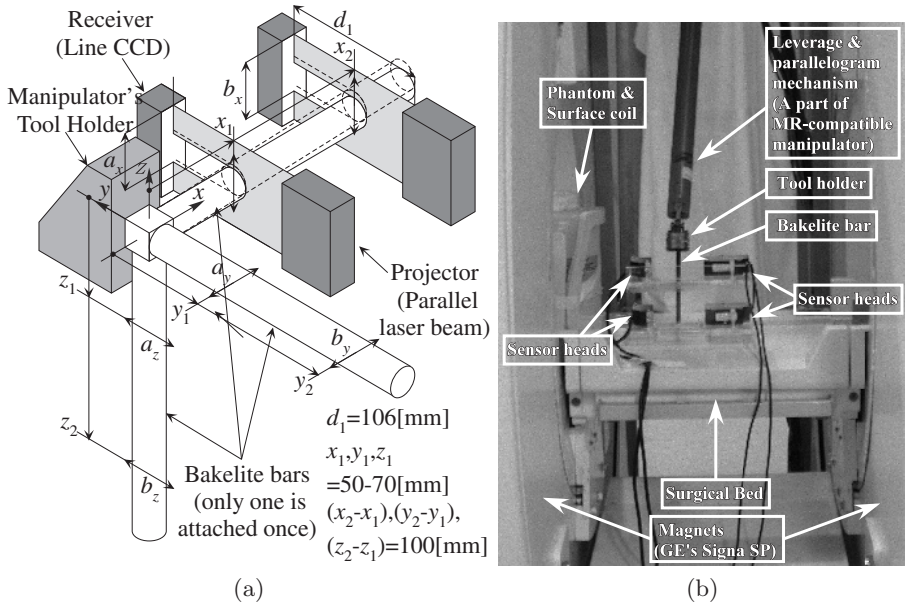


Fig. 2. Setup of the repeatability tests of MR-compatible manipulator: (a) the arrangement of bakelite bars and sensor heads around the manipulator’s tool holder, (b) the arrangement of MR-compatible robot arm, sensor heads, bakelite bar, surface coil and phantom inside the gantry of GE’s intraoperative MRI

$$E_q = STDEV \left(\tan^{-1} \left(\frac{b_x - a_x}{x_2 - x_1} \right) \right) \quad (1)$$

$$E_z = STDEV \left(\frac{b_x - a_x}{x_2 - x_1} (-x_1) + a_x \right) \quad (2)$$

The manipulator moved the bakelite bar to a specific measurement point from the neighboring random point, and the position of the bar was measured in above-mentioned manner. This procedure was repeated 30 times. After that, the bar’s direction was changed to y -axis and z -axis, and x -axis positions and y -axis positions were measured each time. The series of measurement were performed at 5 points, $(x, y, z) = (-60, -60, -60), (60, -60, -60), (0, 0, 0), (-60, 60, 60),$ and $(60, 60, 60)$ and all orientations were $(roll, pitch, yaw) = (0, 0, 0)$. While this experiment, any parts of manipulator including the bar didn’t touch with measuring system or surgical bed.

3 Results and Discussion

3.1 Measurement System Pretests

Fig. 3 shows the average and standard deviation of the reference cylinder’s diameter, inside MRI with image sequence, inside MRI without image sequence, outside MRI, and the average through all conditions.

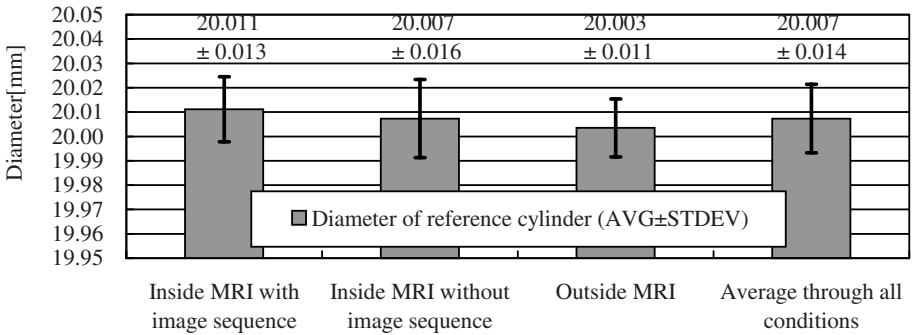


Fig. 3. The average and standard deviation of the reference cylinder’s diameter, measured inside MRI with image sequence, inside MRI without image sequence, and outside MRI.

The averages and standard deviations of each condition were slightly different. The results showed that image sequence didn’t increase the standard deviation, and that outside MRI, the cylinder measured smaller than inside MRI. However, the standard deviation through all conditions, 0.014[mm] was small in comparison with the positioning error of manipulator.

The possible factors of the difference were the influence of MRI and image sequence, incomplete roundness of the cylinder, and setting of sensor heads and the cylinder. It must be noted that not only electric and/or magnetic influence on measuring systems, but also geometrical imprecision, such as roughness of surgical bed, imprecision of mounting block makes geometrical measurement difficult inside MRI.

This pretest concluded that the MRI’s influence on the CCD laser micrometer was negligible, and that the CCD laser micrometer was adequate as the reference of the repeatability test of the MR-compatible manipulator inside MRI.

3.2 Repeatability Tests of MR-Compatible Manipulator

Fig. 4 shows the translational and rotational positioning errors of the MR-compatible leverage and parallelogram manipulator, inside MRI with image sequence, inside MRI without image sequence, outside MRI, and average through all conditions. The errors of each condition were the averages of 5 points. The error ranges were standard deviations of 5 points.

The differences of rotational error between the conditions were minor. The differences of translational error between the conditions were relatively large. The repeatability inside MRI without image sequence was the best and that outside MRI was the worst.

The major possible factors of the error difference between the conditions were the influence of MRI and image sequence on the measuring system and manipulator, setting of the manipulator, bakelite bars, and acrylic block. The results of rotational error indicated that MRI or image sequence didn’t influence the

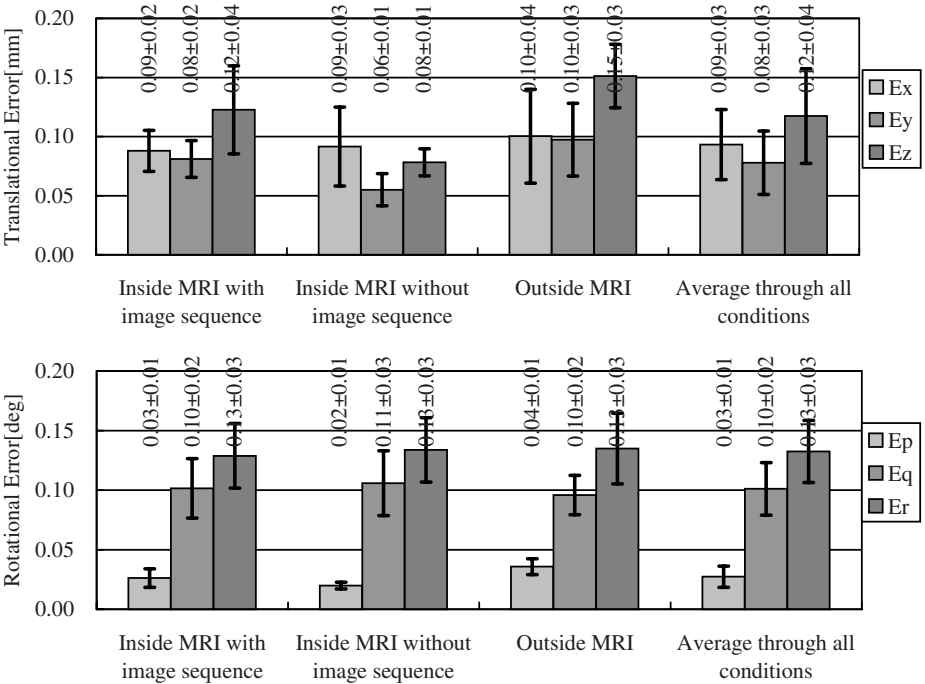


Fig. 4. Translational(upper) and rotational(lower) positioning errors of the MR-compatible leverage and parallelogram manipulator, inside MRI with image sequence, inside MRI without image sequence, outside MRI, and average through all conditions

rotational repeatability. In case of this MR-compatible leverage and parallelogram manipulator, the rotational error and translational error are correlated, because the combination of 6 similar linear driving units determines the position and orientation. Therefore those led that MRI or image sequence didn't influence the translational or rotational repeatability. The rotational error depends on relatively precise parameters (See Eq. (1)). However, the translational error depends on relatively imprecise parameters (See Eq. (2)). So the difference of translational error between the conditions was mainly caused by setting of measuring systems. This experiment indicated that the method to measure the rotational error was precise and adequate to judge if the MRI's influence on the positioning error was minor or not. The method to measure the translational error was relatively imprecise and needs improvement.

In case of rotational repeatability, the order of better repeatability was clear - x-axis was 0.03[deg], y-axis 0.10[deg], and z-axis 0.13[deg] on average through all conditions. The root sum square of average rotational error over all axes was 0.17[deg]. In case of translational repeatability, the order of better repeatability was made unclear by the error of measurement system. The root sum square of average translational error over all axes was 0.17[mm].

4 Conclusion

The engineering significance of this paper is that we have studied how to test the positioning repeatability of MR-compatible manipulator inside MRI. Our method consists of validation of MR-compatibility of measuring system and measurement of the manipulator's repeatability.

Firstly, a CCD laser micrometer was tested to see if it can measure a specimen similarly regardless to inside or outside MRI. The results were different from those outside MRI but the differences were small in comparison with positioning error of manipulator.

Secondly, with this measuring system, the positioning repeatability of our MR-compatible manipulator was tested inside MRI with image sequence, inside MRI without image sequence, and outside MRI. This experiment indicated that the method to measure the rotational error was precise and adequate to judge if the MRI's influence on the positioning error was minor. The method to measure the translational error was relatively imprecise and needs improvement. The results proved that the manipulator performed 0.17[mm] translational and 0.17[deg] rotational positioning repeatability on average, whether inside or outside MRI, whether with or without image sequence.

Acknowledgments. In Japan, this research has been funded by NEDO grant #02A47019b and AIST. In the USA, this research has been funded by NIH grant #P41RR013218, #P01CA067165, and ERC grant #9731748.

We wish to thank Mr. Daniel Kacher for the contribution to this research, as well as the technologists and support staffs of SPL and MRT.

References

1. Masamune K., Kobayashi E., Masutani Y., Suzuki M., Dohi T., Iseki H., Takakura K.: Development of an MRI-compatible needle insertion manipulator for stereotactic neurosurgery. *Journal of Image Guided Surgery*. **1(4)** (1995) 242–248
2. Chinzei K., Kikinis R., Jolesz F.A.: MR Compatibility of Mechatronic Devices: Design Criteria. *Proc. of MICCAI'99*, (1999) 1020–1031
3. Chinzei K., Hata N., Jolesz F.A., Kikinis R.: MR Compatible Surgical Assist Robot System Integration and Preliminary Feasibility Study. *Proc. of MICCAI 2000* 921–930
4. Koseki Y., Koyachi K., Arai T., Chinzei K.: Remote Actuation Mechanism for MR-compatible Manipulator Using Leverage and Parallelogram, Workspace Analysis, Workspace Control, and Stiffness Evaluation. *Proc. of ICRA2003* 652–657
5. Koseki Y., Washio T., Chinzei K., Iseki H.: Endoscope Manipulator for Trans-nasal Neurosurgery, Optimized for and Compatible to Vertical Field Open MRI. *Proc. of MICCAI 2002* 114–121
6. Kaiser W.A., Fischer H., Vagner J., Selig M.: Robotic system for Biopsy and Therapy in a high-field whole-body Magnetic-Resonance-Tomograph. *Proc. Intl. Soc. Mag. Reson. Med.* **8** (2000), 411